Pérez-Benito, C.; Morillas, S.; Jordan-Lluch, C.; Conejero, JA. (2018). A model based on local graphs for colour images and its application for Gaussian noise smoothing. Journal of Computational and Applied Mathematics. 330:955-964. https://doi.org/10.1016/j.cam.2017.05.013

A model based on local graphs for colour images and its application for Gaussian noise smoothing

Cristina Pérez-Benito [a], Samuel Morillas [b,2], Cristina Jordán [c], J. Alberto Conejero [b,*]

[a] *Instituto de Biomecánica de Valencia, Universitat Politècnica de València, E-46022 Valencia, Spain.*

[b] *Instituto Universitario de Matemática Pura y Aplicada, Universitat Politècnica de València, E-46022 Valencia, Spain.*

[c] *Instituto Universitario de Matemática Multidisciplinar, Universitat Politècnica de València, E-46022 Valencia, Spain.*

Abstract

In this paper, a new model for processing colour images is presented. A graph is built for each image pixel taking into account some constraints on links. Each pixel is characterized depending on the features of its related graph, which allows to process it appropriately. As an example, we provide a characterization of each pixel based on the link cardinality of its connected component. This feature enables us to properly distinguish flat image regions respect to edge and detail regions. According to this, we have designed a hybrid filter for colour image smoothing. It combines a filter able to properly process flat image regions with another one that is more appropriate for details and texture. Experimental results show that our model performs appropriately. We also see that our proposed filter is competitive with respect to state-of-the-art methods. It is close closer to the corresponding optimal switching filter respect to other analogous hybrid method.

Key words: Colour Image Processing, Graph Model, Image Smoothing, Hybrid Filter

* Corresponding author
Email address: aconejero@mat.upv.es (J. Alberto Conejero).

[1] Samuel Morillas acknowledges the support of grant MTM2015-64373-P (MINECO/FEDER, UE).
[2] Cristina Jordán acknowledges the support of grant TEC2016-79884-C2-2-R.

1 Introduction

Image denoising is a topic that has been extensively studied in computer vision and digital image processing fields. The denoising (or filtering) step is essential for almost every computer vision system because noise can significantly affect the visual quality of images, as well as the performance of most image processing tasks. Also, in the last years the use of colour images has gained much attention within the computer vision field and therefore colour image denoising has become an important research topic [1].

Among the different sources of noise in digital imaging, probably the most common one is the so-called *thermal noise*, which is due to CCD sensor malfunction. This kind of noise is modeled as an additive white Gaussian noise. So that, the presence of thermal (or Gaussian) noise can be simulated by adding random values from a zero-mean Gaussian distribution to the original values of each image channel independently. The standard deviation σ of the Gaussian distribution characterizes the noise intensity [2]. Many methods for reducing image Gaussian noise in colour images have been proposed in the literature. We will review some of them.

The earliest approaches for Gaussian noise smoothing were based on linear approaches. These methods, such as the *Arithmetic Mean Filter* (AMF), see for instance [2], are able to suppress noise because they take advantage of its zero-mean property. However, they tend to blur edges and texture significantly. This fact motivated the development of many nonlinear methods that try to overcome these drawbacks by detecting image edges and details. This is intended for smoothing there less than in the rest of the image.

Within nonlinear methods, many of them use averaging to take advantage of the zero-mean property of the noise. This class includes the well-known *Bilateral Filter* (BF) [6] and its variants [7]-[11]. Besides, in [12,13] the authors use an averaging operation which is restricted to the *(fuzzy) peer group* members for each image pixel. Other methods are developed using fuzzy logic or soft switching methods, such as those in [14]-[23]. Several methods based on different optimizations of weighted averaging are proposed in [24]-[27]. Another important family of filters are partition based filters [27]-[29], that classify each pixel to be processed into several signal activity categories which, in turn, are associated to appropriate processing methods. Other filters follow a regularization approach [30]-[40] based on the minimization of appropriate energy functions by means of Partial Differential Equations (PDEs). Wavelet theory has also been used to design image filtering methods [41]-[50]. The combination of collaborative non-local means and wavelet filtering is proposed in [51,52], and a method using the wavelet transformation and data regularization is proposed in [53]. Other recent methods make use of a combination of

image analysis techniques for image segmentation followed by an appropriate smoothing of each image region [54]-[56]. More recently, methods using graph modeling colour images have provided competitive filtering solutions as [57,58].

Despite that many works have consider this question up to date, the problem remains open. Recently, very few works have been published (just 2 articles [58,40] in prestigious journals in four years, 2013-2016). This is due, in part, to new image models being needed to develop new filtering solutions. Therefore, in this paper we propose a new model for colour images which is based on graph theory and vector processing. In the model, a local graph is built for each image pixel taking into account some constraints on links. Each pixel is characterized depending on the features of its related graph so that it can be properly processed. As an application of the model, we provide a characterization of each pixel based on the link cardinality of its connected component. This feature is able to properly distinguish flat image regions respect to edge and detail regions. According to this characterization, we have designed a hybrid filter for colour image smoothing that combines a filter able to properly process flat image regions with another one more appropriate for details and texture. This approach follows the methodology in [23,57]. The experimental results show that the proposed filter is competitive with analogous filters and closer to the corresponding optimal soft-switching filter.

The paper is organized as follows: Section 2 described the local graph model for colour images, Section 3 details the pixel characterization, and Section 4 introduces the hybrid filter. Finally, experimental results and conclusions are given in Sections 5 and 6, respectively.

2 Image model based on local graphs

A graph G is defined as a finite nonempty set $V(G)$ of objects called *vertices* and a set $L(G)$ of unordered pairs of distinct vertices of G which, in order to avoid confusion with the image processing terminology, we will call *links* instead of edges, as it is common practice. Two vertices u and v joined by a link (u, v) are said to be *adjacent*. When each link (u, v) has an associated value $w(u, v)$, we say that the graph is *weighted*.

A graph H is called a subgraph of G if $V(H) \subseteq V(G)$ and $L(H) \subseteq L(G)$. A walk W from a node v_0 to a node v_l in a graph is a sequence of vertices say $v_0, v_1, \ldots, v_l$ where $(v_{i-1}, v_i) \in L(G)$, $0 < i \leq l$. A graph is *connected* if for every pair v_i, v_j of distinct vertices there is a walk from v_i to v_j.

A connected component of a nondirected graph G is a connected subgraph H

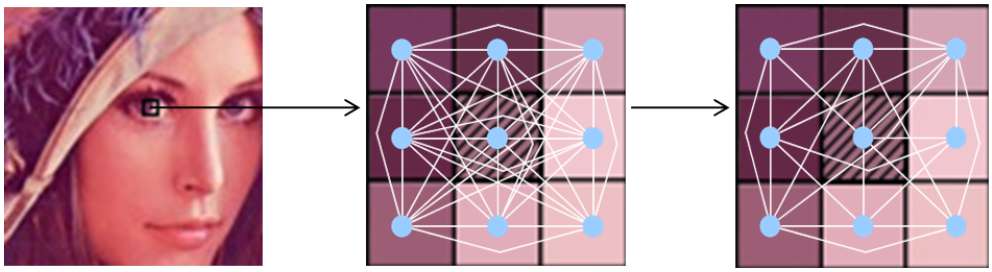

Fig. 1. Example of 3x3 window in an image (left) and its associated graph with all the links (center), and with the links lower than the threshold $\mathcal{U}$ (right) that is $G_{\mathbf{F}_0}$.

of G such that there is not a connected subgraph of G that contains H strictly.

For a colour image $\mathbf{F}$, which is represented in the RGB colour space, we build a graph-based model for each pixel in $\mathbf{F}$. In doing so, we take the neighbours around each image pixel $\mathbf{F}_0$ in a window centered on it of size $N \times N$ where $N = 2n + 1$ and $n = 1, 2, \ldots$. The rest of the neighbour pixels in the window are denoted as $\mathbf{F}_i, i = 1, \ldots, N^2 - 1$. The central pixel $\mathbf{F}_0$ is in turn defined by the tern (F_0^R, F_0^G, F_0^B) of its three RGB colour components. In the following we will use $n = 1$ as it is common practice in colour image filtering.

Given a pixel $\mathbf{F}_0$, we define a local weighted graph $G_{\mathbf{F}_0}$ where $V(G_{\mathbf{F}_0}) = \{\mathbf{F}_i,\, i = 0, \ldots, N^2 - 1\}$ and $L(G_{\mathbf{F}_0}) = \{(\mathbf{F}_i, \mathbf{F}_j),\, i \neq j,\, ||\mathbf{F}_i - \mathbf{F}_j||_2 < \mathcal{U}\}$. That is, a link exists between pixel $\mathbf{F}_i$ and $\mathbf{F}_j$, $i \neq j$, if the euclidean distance between their colour vectors is lower than a certain threshold $\mathcal{U}$. If such a link exists, its weight is $w(\mathbf{F}_i, \mathbf{F}_j) = ||\mathbf{F}_i - \mathbf{F}_j||_2$, where $||\cdot||$ stands for the Euclidean norm, see the example in Figure 1.

The value of $\mathcal{U}$ critically influences the structure of each local graph since it determines the connected component of $G_{\mathbf{F}_0}$ that contains the node $\mathbf{F}_0$, noted as $H_{\mathbf{F}_0}$. This connected component will play an important role in order to classify the different regions of the image into flat or detail/texture regions. We will discuss extensively the adjustment of the threshold $\mathcal{U}$ in the following section. Our global image model is the composition of all local graphs that characterize each image pixel.

3 A characterization of colour image pixels for smoothing

As an example of application of our model we aim to develop a procedure for smoothing colour images. To this end, it is critical to distinguish flat image regions in front of edges and details. This is because optimal smoothing needs to process differently flat regions, where smoothing can be more aggressive, from texture and detail regions, where smoothing should be done with special care. So, we need to devise a characterization based on our model to make

(a) Lenna (b) Parrots (c) Statue (d) Peppers

Fig. 2. Set of training images

Fig. 3. Grayscale image where intensity of each pixel is proportional to $\mathbf{card}(L(H_{\mathbf{F}_0}))$.

such a classification.

We have seen that the feature that better characterizes whether a pixel $\mathbf{F}_0$ belongs to a flat or edge/detail region is the cardinal of the links set of its connected component, $\mathbf{card}(L(H_{\mathbf{F}_0}))$. Lower cardinality is associated to texture, edges and details whereas higher values correspond to flat image regions, as we can see if we compare the images in Figure 3, that were created assigning grayscale image levels proportional to $\mathbf{card}(L(H_{\mathbf{F}_0}))$, with the corresponding original images in Figure 3, that were created assigning grayscale image levels proportional to $\mathbf{card}(L(H_{\mathbf{F}_0}))$, with the corresponding original images shown in Figure 2.

However, for this characterization to be as accurate as possible it is critical to properly set the value of $\mathcal{U}$ for each input image. We have applied a method for this as follows.

3.1 Adjustment of $\mathcal{U}$ parameter

The role of $\mathcal{U}$ is to avoid that very different pixels in the image were connected. In the context of image smoothing, we have to find a setting that is robust to the presence of noise or at least we need to adapt it to the density of contaminating noise. Given that the feature that better characterizes whether a pixel $\mathbf{F}_0$ belongs to a flat or detail region is $\mathbf{card}(L(H_{\mathbf{F}_0}))$, we focus the adjustment of $\mathcal{U}$ to maximize the correlation between $\mathbf{card}(L(H_{\mathbf{F}_0}))$ and the presence of edges/texture.

Therefore, we first have taken the four training colour images in Figure 2 and for each of them we have obtained a groundtruth image of edges by means

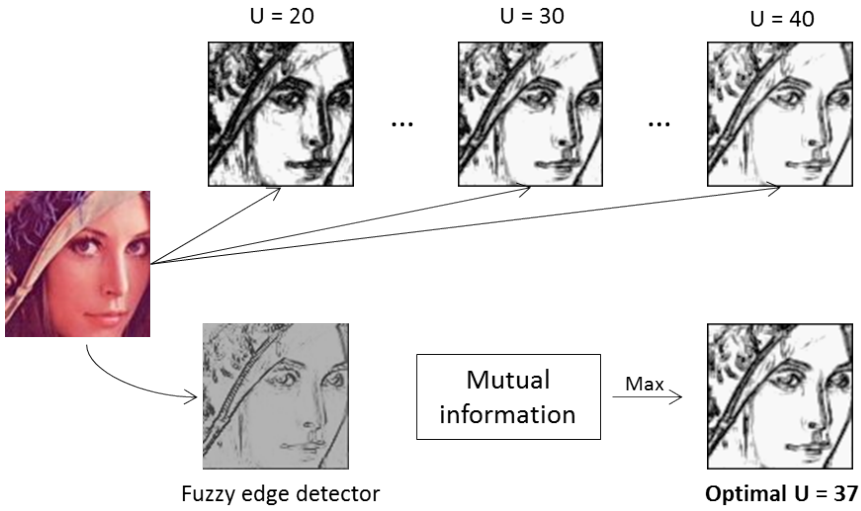

Fig. 4. Scheme of the method for set the optimal threshold $\mathcal{U}$

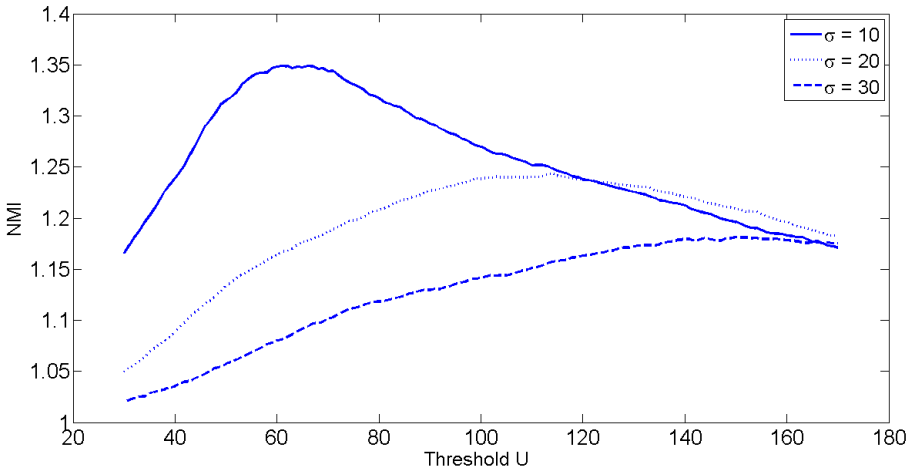

Fig. 5. NMI as a function of $\mathcal{U}$ for Parrots with different levels of noise

of the fuzzy edge detection method [64] as it is implemented in MATLAB© R2016b.

Secondly, for each noise free training image we have computed the value of $\mathcal{U}$ that maximizes the images mutual information (NMI) [62,63] between the grayscale image obtained with the $\mathbf{card}(L(H_{\mathbf{F}_0}))$ of each pixel and the corresponding groundtruth image of the first step. Then, using each optimal value of $\mathcal{U}$ and the values $\mathbf{card}(L(H_{\mathbf{F}_0}))$ we obtain four edge/texture reference images that we use in the next step.

Thirdly, since our method will process noisy images with unknown noise variance, it would be desirable to have robustness against noise or at least adaptiveness to noise. So that, we have contaminated the training colour images with different densities of additive white Gaussian noise ($\sigma \in \{10, 20, 30\}$)

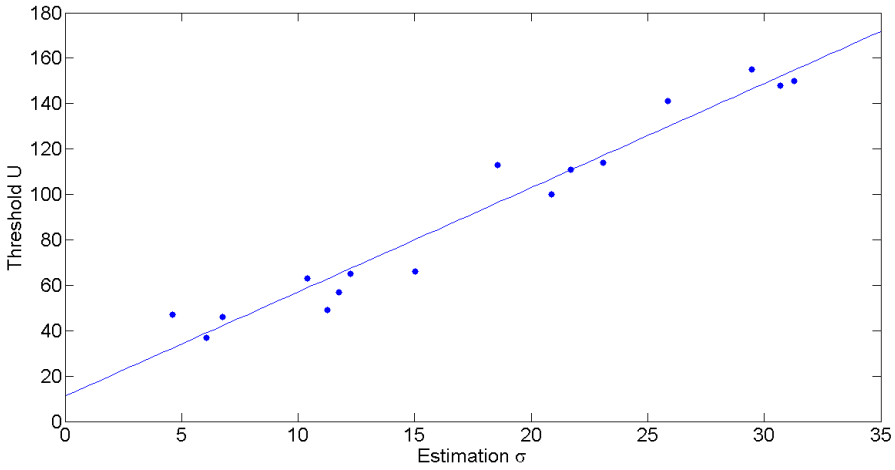

Fig. 6. Regression bewteen the estimation of the noise and the optimal threshold

according to the model in [2]. For each of the 12 noisy images we obtain the value of $\mathcal{U}$ that maximizes the NMI between the grayscale image obtained with the $\mathbf{card}(L(H_{\mathbf{F}_0}))$ of each pixel and the corresponding edge/texture reference image of the second step. It can be seen in Figure 5 that the higher the image noise is, the greater the optimal threshold is, too. Finally, we have conducted a linear regression analysis over all optimal $\mathcal{U}$ to be able to appropriately set $\mathcal{U}$ for any input image. We have also used an estimation of the standard deviation of the noise, $\hat{\sigma}$, in the input image, which is obtained using the method in [61] (we average the estimate in each of the RGB channels). The regression, that can be seen graphically in Figure 6, concludes that we can safely set $\mathcal{U}$ as

$$\mathcal{U} = 4.59\hat{\sigma} + 11.16, \tag{1}$$

given that correlation coefficient r equals 0.9187. The scheme in Figure 4 summarizes the procedure applied.

4 Proposed hybrid smoothing method

Recent smoothing methods commonly present the drawback that, as the higher the noise in the image is, the more confused is the noise in homogeneous regions with the image structure that should be preserved. So that, it cannot be properly reduced.

There are some filtering structures more suitable for smoothing, and others more powerful for preserving borders. We take, for instance, one filter of each type: AMF to process image flat regions and the nonlinear method called

Fuzzy Noise Reduction Method (FNRM) [15] FNRM for the rest of the image. We propose to combine them following the reasoning in [57].

The switching between AMF and FNRM is performed in a soft fashion so that when the class of the image pixel is not clearly determined the results of both methods are combined. The proposed filter follows the idea behind the *Soft-Switching Graph Denoising* (SSGD) method in [57], but using our new model and characterization based on $\mathbf{card}(L(H_{\mathbf{F}_0}))$. In addition, notice that although we have used the AMF and FNRM, any other methods can be used within the same structure and analogous improvements are expected.

The combination of the aforementioned methods is performed as follows: Let us consider a pixel $\mathbf{F}_0$. Since $L(H_{\mathbf{F}_0})$ is a connected component of $G_{\mathbf{F}_0}$, the parameter $\mathbf{card}(L(H_{\mathbf{F}_0}))$ takes discrete values, between 0 and $\binom{N^2}{2}$. In our case $N = 3$ and

$$\mathbf{card}(L(H_{\mathbf{F}_0})) \in \{0, \ldots, 36\}, \tag{2}$$

We classify the image pixels of any image into one of these 37 different categories, one for each admissible value of $\mathbf{card}(L(H_{\mathbf{F}_0}))$. In this way, we build $\beta = \{\beta_1, \ldots, \beta_{37}\}$, with $0 \leq \beta_i \leq 1$. If $\mathbf{card}(L(H_{\mathbf{F}_0})) = i - 1$, we make $\mathbf{F}_0$ in correspondence with β_i. These values $\beta_i' s$ shall determine the soft-switching between AMF and FNRM to process each image pixel.

This new method will be called a *Soft-Switching Local Graph Denoising* method (SSLGD). For each image pixel $\mathbf{F}_0$, if $\mathbf{card}(L(H_{\mathbf{F}_0})) = i$, the output of SSLGD is

$$SSLGD_{out}(\mathbf{F}_0) = (1 - \beta_i) AMF_{out}(\mathbf{F}_0) + \beta_i FNRM_{out}(\mathbf{F}_0) \tag{3}$$

where $\beta_i \in [0, 1]$.

Notice that when $\beta_i = 1$ the $SSLGD$ method behaves as the $FNRM$, and when $\beta_i = 0$ it coincides with the AMF. Thus, the value of β_i should depend on the nature of the pixel under process. Therefore, if the pixel $\mathbf{F}_0$ belongs to an homogeneous region of the image β_i should be large (close to 1), otherwise, β_i should be lower (close to 0).

In this method it is critical to find a setting for the values β_i in equation (3) in order to obtain the better combination between AMF and FNRM. To do it we use the ascending gradient method for maximizing the *Peak Signal to Noise Ratio* (PSNR) [2] between the filter output and the original noise free image. In this optimization we have used as initial vector $B^0 = (\beta_i^0)$, where $\beta_i^0 = 1$, and a step $\delta = 0.05$. We find the optimization for the 4 training images each of them contaminated with 3 different densities of noise ($\sigma \in \{10, 20, 30\}$) which provides 12 optimized sets of β_i's.

Now, by using these sets we compute three default sets of $\beta = (\beta_i)_{1\leq i\leq 37}$'s, one for low noise ($\beta^{10}, \sigma = 10$), another for medium noise ($\beta^{20}, \sigma = 20$) and a third one for high noise ($\beta^{30}, \sigma = 30$). To process an input image where noise is unknown we use the noise estimation $\hat{\sigma}$ and we choose among $\beta^{10}, \beta^{20}, \beta^{30}$ the set with superscript closest to $\hat{\sigma}$, that we call it now $\bar{\beta}$. The choice of $\bar{\beta}$ for each image is determined by the noise estimation. In this sense, if the estimation of noise level is the same for two images, they will be processed analogously, but two images having the same real noise level may have different estimation of noise. As we have said before, the noise is unknown in general, thus using a noise estimator provide us a more realistic and robust approach when processing any image.

Although it is true that using more images makes better the learning, the inclusion of more images will adjust the values in a unnecessary precision since the step of βs in the optimization is δ= 0.05 and then the differences in the ranges in which we move are imperceptible. For this reason and taking into account that our goal is to find an appropriate general robust setting that could be used to process any unknown image, we consider four images, with different structures that provide us enough information for set the beta values in a general way.

Notice that we have chosen a window size 3×3. According to previous works [65,66], using $N > 3$ results in higher noise smoothing capability but much more blurred images that make increasing the window not a good choice in general. If the interest is to increase noise reduction capability, it has been reported to be a much better choice to apply several iterations of the same method, that is, filtering the output image again and again until convergence is reached.

5 Experimental results

In this section, we compare the performance of the SSLGD filter respect to other filters with the aim of validating the parameter settings. In Figure 7, we show the validation set of images. We have added Gaussian noise with standard deviations $\sigma \in \{10, 20, 30\}$ to them, obtaining an experimental set of 12 images.

We process all 12 images with SSLGD using two different parameter setting for $\mathcal{U}$ and β: one with the optimal settings for the particular image and noise $\mathcal{U}_{op}, \beta_{op}$ which we denote by $SSLGD_{\mathcal{U}_{op},\beta_{op}}$, and another with the estimated $\mathcal{U}_e$ and $\bar{\beta}$ which we denote by $SSLGD_{\mathcal{U}_e,\bar{\beta}}$. We compare the performance for the experimental set of images with respect to the methods AMF, FNRM, and SSGD, which is a method following the same structure of SSLGD. In addition,

(a) Micro (b) Pills (c) Window (d) img58

Fig. 7. Images used for the validation.

we compare with the optimal hybrid method associated to SSLGD and SSGD that we call *Optimal Soft Switching* (OSS), and which is defined as the best combination between AMF and FNRM, defined for each pixel $\mathbf{F}_0$ by:

$$OSS_{out}(\mathbf{F}_0) = \alpha_i AMF_{out}(\mathbf{F}_0) + (1-\alpha_i) FNRM_{out}(\mathbf{F}_0) \qquad \alpha_i \in [0,1] \quad (4)$$

where $\alpha_i = argmin_{[0,1]}||\mathbf{F}_0 - OSS_{out}(\mathbf{F}_0)||, i \in \{0,1,\ldots,36\}$ can be easily derived analytically if the original image $\mathbf{F}$ is known.

As figures of merit for objective evaluation we have used the PSNR, SSIM [60], and the *Fuzzy Colour Structural Similarity* [59], denoted by FCSS. These latter two methods have proved to correlate with human perception better than PSNR.

	σ	10			20			30		
		PSNR	**FCSS**	**SSIM**	**PSNR**	**FCSS**	**SSIM**	**PSNR**	**FCSS**	**SSIM**
Micro	AMF	28.430	0.890	0.775	27.147	0.889	0.694	25.580	0.884	0.606
	FNRM	31.334	**0.943**	0.866	27.964	**0.925**	0.741	25.216	0.902	0.617
	SSGD	**31.34**	**0.943**	**0.867**	28.06	**0.925**	0.746	25.63	0.907	0.634
	$SSLGD_{\beta_{op},\mathcal{U}_{op}}$	**31.34**	**0.943**	**0.867**	**28.36**	0.920	0.752	26.05	**0.908**	0.648
	$SSLGD_{\bar{\beta},\mathcal{U}_e}$	31.154	0.936	0.865	28.333	0.918	**0.754**	**26.097**	0.907	**0.65**
	OSS	**32.218**	**0.95**	**0.891**	**29.788**	**0.942**	**0.810**	**27.638**	**0.933**	**0.728**
Pills	AMF	25.913	0.888	0.885	25.211	0.882	0.856	24.139	0.874	0.809
	FNRM	32.417	0.944	0.962	28.143	0.919	0.901	25.138	0.891	0.825
	SSGD	32.62	0.945	0.966	28.89	0.925	0.921	**26.59**	0.907	**0.862**
	$SSLGD_{\beta_{op},\mathcal{U}_{op}}$	**32.69**	**0.946**	**0.967**	**28.97**	**0.926**	**0.923**	26.28	**0.909**	0.864
	$SSLGD_{\bar{\beta},\mathcal{U}_e}$	32.26	0.943	0.965	28.70	0.923	0.919	26.14	0.907	0.860
	OSS	**34.433**	**0.961**	**0.978**	**30.81**	**0.947**	**0.948**	**28.07**	**0.933**	**0.903**
Window	AMF	22.36	0.832	0.715	22.00	0.834	0.689	21.42	0.833	0.650
	FNRM	31.13	0.930	0.946	27.46	0.912	0.878	24.59	0.889	0.802
	SSGD	31.14	0.929	0.94	27.4	0.91	0.873	24.65	0.892	0.8
	$SSLGD_{\beta_{op},\mathcal{U}_{op}}$	**31.21**	**0.931**	**0.951**	**27.67**	**0.916**	**0.889**	**24.96**	**0.897**	**0.815**
	$SSLGD_{\bar{\beta},\mathcal{U}_e}$	30.34	0.92	0.95	26.93	0.906	0.879	24.47	0.888	0.792
	OSS	**32.87**	**0.946**	**0.965**	**29.59**	**0.936**	**0.925**	**27.05**	**0.925**	**0.7877**
img58	AMF	27.78	0.912	0.831	26.58	0.908	0.746	25.29	0.898	0.659
	FNRM	33.06	0.946	0.904	28.32	0.911	0.750	25.28	0.869	0.622
	SSGD	33.24	**0.958**	0.905	29.38	**0.931**	0.77	26.69	**0.911**	0.67
	$SSLGD_{\beta_{op},\mathcal{U}_{op}}$	**33.45**	0.947	0.9156	**29.42**	0.93	**0.804**	**26.77**	**0.911**	**0.70**
	$SSLGD_{\bar{\beta},\mathcal{U}_e}$	33.04	0.946	0.899	28.68	0.922	0.74	25.90	0.889	0.599
	OSS	**35.27**	**0.962**	**0.946**	**31.16**	**0.949**	**0.861**	**28.56**	**0.936**	**0.780**

Table 1: Results in terms of PSNR, SSIM and FCSS of the validation set.

	σ	10		20		30	
		PSNR	**SSIM**	**PSNR**	**SSIM**	**PSNR**	**SSIM**
Window	SSGD	36.78	0.989	33.55	0.972	31.67	0.949
	$SSLGD_{\bar{\beta},\mathcal{U}_e}$	37.66	0.989	33.64	0.971	31.11	0.951
img58	SSGD	39.51	0.977	36.88	0.965	33.96	0.945
	$SSLGD_{\bar{\beta},\mathcal{U}_e}$	40.33	0.982	35.04	0.941	31.74	0.900
Micro	SSGD	40.60	0.982	35.18	0.945	33.62	0.915
	$SSLGD_{\bar{\beta},\mathcal{U}_e}$	41.86	0.983	37.83	0.967	35.42	0.948
Pills	SSGD	38.44	0.991	35.27	0.983	33.02	0.974
	$SSLGD_{\bar{\beta},\mathcal{U}_e}$	39.83	0.992	36.44	0.985	34.123	0.978

Table 2: Results in terms of PSNR and SSIM comparing with OSS

From the results in Table 1 we can see that both in terms of PSNR, FCSS and SSIM the performance of $SSLGD_{\bar{\beta},\mathcal{U}_e}$ is very close to $SSLGD_{\beta_{op},\mathcal{U}_{op}}$. This

means that the methods for parameter setting are performing appropriately. Also, we see that the performance of our method is competitive with SSGD and both SSGD and SSLGD are a little bit below OSS, which implies that the proposed method is competitive with respect to state-of-the-art methods.

To see which of SSGD or SSLGD is closer to the optimal OSS we have also computed the PSNR and SSIM for SSGD and SSLGD with respect to OSS. These results are shown in Table 5, where we can see that SSLGD is close to the optimal OSS, which is a strong point for our method and the model behind it. We consider that this comparation is more important than the one in Table 1, since the original image is irretrievable and OSS image is the maximum to what can be reached with this kind of hybrid filter.

In Figure 8 we can see the qualitative results of AMF, FNRM, SSGD and the new proposed filter SSLGD. They have been applied separately to the set of validation images with standard deviation $\sigma = 20$.

As it can be seen, on the one hand AMF smooths the noise fine but it blurs the image. On the other hand, we can see how in all the cases FNRM does not blur the image. However, it does not remove so much noise. SSGD improves this drawback combining both methods and achieving a good denoising without blurring the image. Finally, our propose method follows the line of SSGD, being very close to it. The differences between both methods can be appreciated in detail regions such as the blinds of Window, or the edges of the capsules of Pills.

Although the result of SSLGD is close to SSGD, it can be seen more globally as the result of SSLGD is closer to OSS image than the SSGD, what is the most important for us, being especially appreciated in the homogeneous regions.

5.1 Computational Complexity

We will analyze the computational complexity of the proposed method and SSGD for each pixel of the image. The number of operations for each pixel depends on the window NxN considered, a total of N^2 pixels in the window. Since both methods depend on two basic generic filters, one for homogeneous regions and other for borders regions, we will focus on the complexity of SSLGD and SSGD. We denote the computational complexity of the homegeneous-regions and detail-regions generic filters as $H(N^2)$ and $E(N^2)$, respectively.

In the proposed method, for each pixel we have to compute the distance between the central pixel and its neighbours, that is to say, a total of $\frac{N^2(N^2-1)}{2}$ distances, which means $\frac{9N^2(N^2-1)}{2}$ distances in total. Once the distances are cal-

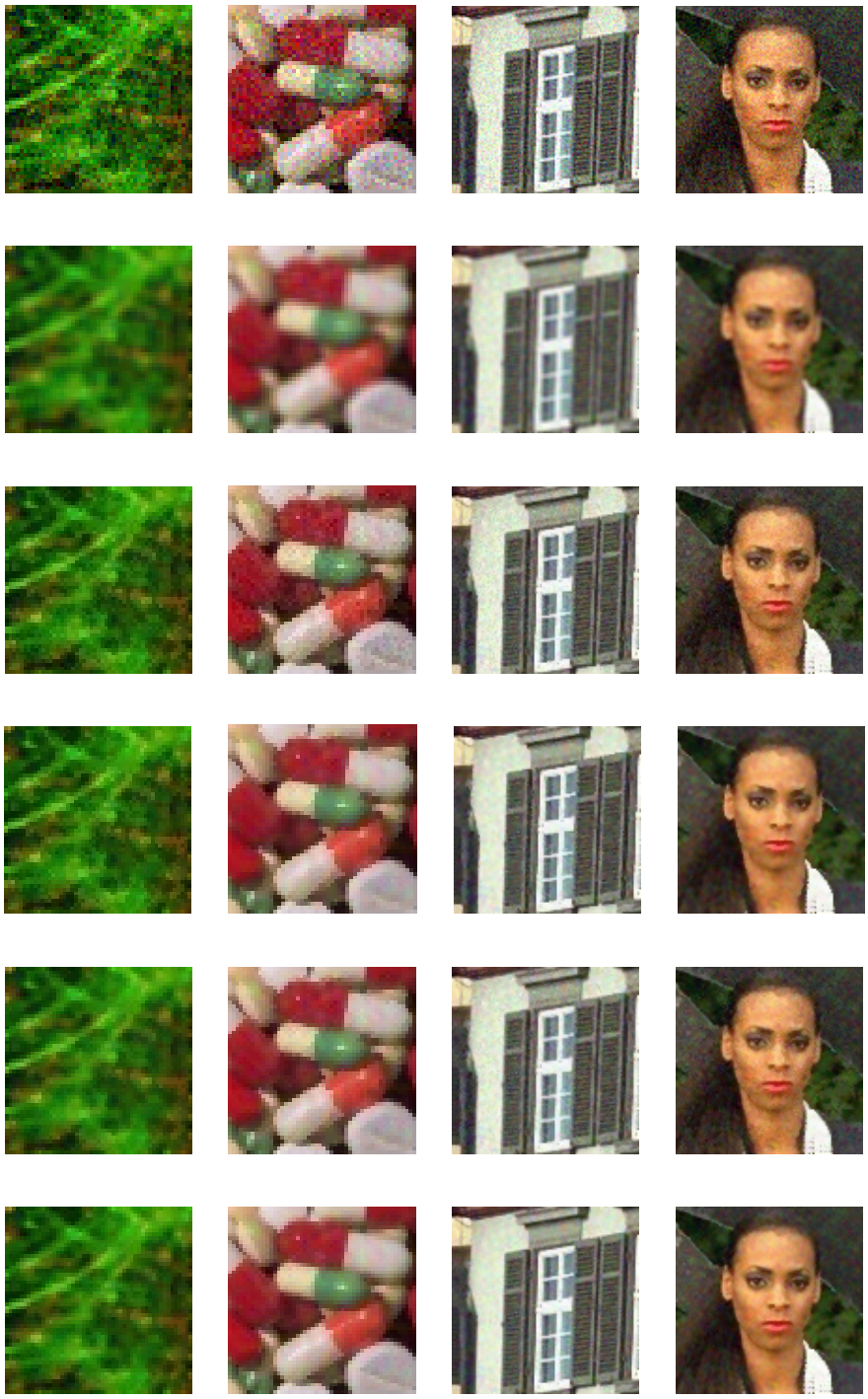

Fig. 8. Filtered image: first row the original images blurred with Gaussian noise with $\sigma = 20$, second row the filtered images using AMF, third row using FNRM, the fourth row with SSGD,the fifth row with SSGLD and finally OSS images.

culated, we compare all of them with the fixed threshold in order to compute $\mathbf{card}(L(H_{\mathbf{F}_0}))$. This would amount to a total of $\frac{N^2(N^2-1)}{2}$ comparisons. In this way, we have a total of $\frac{10N^2(N^2-1)}{2}$ comparisons. The value of $\mathbf{card}(L(H_{\mathbf{F}_0}))$

allows us to choose the corresponding β for combine appropriately the based filters. Thus SSLGD needs a number of operations of order $\mathcal{O}(N^2) + H(N^2) + E(N^2)$.

SSGD filter, as SSLGD do, needs to compute the distances between the central pixel and its neighbours ($\frac{9N^2(N^2-1)}{2}$ operations). Kruskal algorithm, whose computational cost is $\mathcal{O}\left(N^2 \log(N^2)\right)$, is applied twice in order to compute the maximum and minimum spanning tree by considering the mentioned distance. Minimum spanning tree's weight allows to compute the coefficient that will be used in the linear combination of the generic filters. The computational complexity of this method is therefore of order $\mathcal{O}(N^2 \log(N^2)) + H(N^2) + E(N^2)$.

The proposed SSLGD method is computationally more efficient than SSGD. SSLGD has the advantage of having fixed parameters *beta* for processing the pixels. In contrast, SSGD performs all the soft switching mechanism completely for every pixel, which increases the number of operations and the computational time.

6 Conclusions

In this paper, we have presented a new model based on local graphs for low level image processing. In the model, each pixel is associated to a graph whose features allow to characterize it. We show an application of the model for Gaussian noise smoothing which is based on using each pixel graph to decide whether a pixel belongs to a flat region or not. The model allows to distinguish appropriately flat regions and border regions in an image even in the presence of noise. Related to this classification a soft-switching filter is built by using a filter with good smooth capability in flat regions and another to smooth border regions. Also, parameters of the method have been analyzed and it has been proposed how to set them automatically for any input image, so that the filter is very easy to use.

Performance of the new proposed method, SSLGD, in terms of PSNR, SSIM and FCSS shows that it is competitive with respect to state-of-the-art methods, decreasing the computational complexity thanks to the global characterization of the parameters, which allows us to reduce the computational cost. Also, objective comparison with respect to the corresponding optimal hybrid filter claims that our method is closer to the optimal than another soft-switching filter with the same structure.

References

[1] Celebi, M.E., Lecca, M., Smolka, B.: Color Image and Video Enhancement: *Springer-Verlag*, Berlin (2015).

[2] Plataniotis, K.N., Venetsanopoulos, A.N.: Color Image processing and applications. *Springer-Verlag*, Berlin (2000).

[3] Lukac, R., Smolka, B., Martin, K., Plataniotis, K.N., Venetsanopoulos, A.N.: Vector Filtering for Color Imaging, *IEEE Signal Processing Magazine, Special Issue on Color Image Processing*, 22, 74-86 (2005).

[4] Lukac, R., Plataniotis, K.N.: A taxonomy of color image filtering and enhancement solutions.*Hawkes, P.W. (ed) Advances in Imaging and Electron Physics*, 140, pp. 187-264. Elsevier Acedemic Press (2006).

[5] Buades, A., Coll, B., Morel, J.M.: Nonlocal image and movie denoising. *International Journal of Computer Vision*, 76, 123-139 (2008).

[6] Tomasi, C., Manduchi, R.: Bilateral filter for gray and color images. *Proceedings of IEEE International Conference Computer Vision*, 839-846 (1998).

[7] Elad, M.: On the origin of bilateral filter and ways to improve it. *IEEE Transactions on Image Processing*, 11, 1141-1151 (2002).

[8] Kao, W.C., Chen, Y.J.: Multistage bilateral noise filtering and edge detection for color image enhancement. *IEEE Transactionc on Consumer Electronics*, 51, 1346-1351 (2005).

[9] Garnett, R., Huegerich, T., Chui, C., He, W.: A universal noise removal algorithm with an impulse detector. *IEEE Transactions on Image Processing*, 14, 1747-1754 (2005).

[10] Morillas, S., Gregori, V., Sapena, A.: Fuzzy Bilateral Filtering for color images, *Lecture Notes in Computer Science*, 4141, 138-145 (2006).

[11] Zhang, B., Allenbach, J.P.: Adaptive bilateral filter for sharpness enhancement and noise removal. *IEEE Transactions on Image Processing*, 17, 664-678 (2008).

[12] Kenney, C., Deng, Y., Manjunath, B.S., Hewer, G.: Peer group image enhancement. *IEEE Transactions on Image Processing*, 10, 326-334 (2001).

[13] Morillas, S., Gregori, V., Hervás, A.: Fuzzy peer groups for reducing mixed Gaussian-impulse noise from color images. *IEEE Transactions on Image Processing*, 18, 1452-1466 (2009).

[14] Plataniotis, K.N., Androutsos, D., Venetsanopoulos, A.N.: Adaptive fuzzy systems for multichannel signal processing. *The Proceedings of the IEEE*, 87, 1601-1622 (1999).

[15] Schulte, S., De Witte, V., Kerre, E.E.: A fuzzy noise reduction method for colour images. *IEEE Transactions on Image Processing*, 16, 1425-1436 (2007).

[16] Shen, Y., Barner, K.: Fuzzy vector median-based surface smoothing. *IEEE Transactions on Visualization and Computer Graphics*, 10, 252-265 (2004).

[17] Lukac, R., Plataniotis, K.N., Smolka, B., Venetsanopoulos, A.N.: cDNA Microarray Image Processing Using Fuzzy Vector Filtering Framework, *Fuzzy Sets and Systems*, 152, 17-35 (2005).

[18] Smolka, B.: On the new robust algorithm of noise reduction in color images, *Computers & Graphics*, 27, 503-513 (2003).

[19] Van de Ville, D., Nachtegael, M., Van der Weken, D., Philips, W., Lemahieu, I., Kerre, E.E.: Noise reduction by fuzzy image filtering,*IEEE Transaction on Fuzzy Systems*, 11, 429-436 (2003).

[20] Schulte, S., De Witte, V., Nachtegael, M., Van der Weken, D., Kerre, E.E.: Histogram-based fuzzy colour filter for image restoration, *Image and Vision Computing*, 25, 1377-1390 (2007).

[21] Nachtegael, M., Schulte, S., Van der Weken, D., De Witte, V., Kerre, E.E.: Gaussian noise reduction in grayscale images, *International Journal of Intelligent Systems Technologies and Applications*, 1, 211-233 (2006).

[22] Schulte, S., De Witte, V., Nachtegael, M., Mélange, T., Kerre, E.E.: A New Fuzzy Additive Noise Reduction Method. *Lecture Notes in Computer Science*, 4633, 12-23 (2007).

[23] Morillas, S., Schulte, S., Mélange, T., Kerre, E.E., Gregori, V.: A soft-switching approach to improve visual quality of colour image smoothing filters. *Proceedings of Advanced Concepts for Intelligent Vision Systems ACIVS07, Lecture Notes in Computer Science*, 4678, 254-261 (2007).

[24] Lucchese, L., Mitra, S.K.: A new class of chromatic filters for color image processing: theory and applications,*IEEE Transactions on Image Processing*, 13, 534-548 (2004).

[25] Lee, J.A., Geets, X., Grégoire, V., Bol, A.: Edge-preserving filtering of images with low photon counts. *IEEE Transactions on Pattern Analysis and Machine Intelligence*, 30, 1014-1027 (2008).

[26] Russo, F.: Technique for image denoising based on adaptive piecewise linear filters and automatic parameter tuning, *IEEE Transactions on Instrumentation and Measurement*, 55, 1362-1367 (2006).

[27] Shao, M., Barner, K.E.: Optimization of partition-based weighted sum filters and their application to image denoising. *IEEE Transactions on Image Processing*, 15, 1900-1915 (2006).

[28] Ma, Z., Wu, H.R., Feng, D.: Partition Based Vector Filtering Technique for Suppression of Noise in Digital Color Images. *IEEE Transactions on Image Processing*, 15, 2324-2342 (2006).

[29] Ma, Z., Wu, H.R., Feng, D.: Fuzzy Vector Partition Filtering Technique for Color Image Restoration. *Computer Vision and Image Understanding*, 107, 26-37 (2007).

[30] Perona, P., Malik, J.: Scale-space and edge detection using anisotropic diffusion, *IEEE Transactions on Pattern Analysis and Machine Intelligence*, 12, 629-639 (1990).

[31] Sroubek, F., Flusser, J.: Multichannel blind iterative image restoration, *IEEE Transactions on Image Processing* 12, 1094-1106 (2003).

[32] Hu, J., Wang, Y., Shen, Y.: Noise reduction and edge detection via kernel anisotropic diffusion. *Pattern Recognition Letters*, 29, 1496-1503 (2008).

[33] Li, X.: On modeling interchannel dependency for color image denoising. *International Journal of Imaging Systems and Technology, Special issue on applied color image processing*, 17, 163-173 (2007).

[34] Keren, D., Gotlib, A.: Denoising Color Images using regularization and correlation terms. *Journal of Visual Communication and Image Representation*, 9, 352-365 (1998).

[35] Lezoray, O., Elmoataz, A., Bougleux, S.: Graph regularization for color image processing. *Computer Vision and Image Understanding*, 107, 38-55 (2007).

[36] Elmoataz, A., Lezoray, O., Bougleux, S.: Nonlocal discrete regularization on weighted graphs: A framework for image and manifold processing.*IEEE Transactions on Image Processing*, 17, 1047-1060 (2008).

[37] Blomgren, P., Chan, T.: Color TV: total variation methods for restoration of vector-valued images. *IEEE Transactions on Image Processing*, 7, 304-309 (1998).

[38] Tschumperl, D., Deriche, R.: Vector-valued image regularization with PDEs: A Common framework from different applications. *IEEE Transactions on Pattern Analysis and Machine Intelligence*, 27, 506-517 (2005).

[39] Plonka, G., Ma, J.: Nonlinear regularized reaction-diffusion filters for denoising of images with textures, IEEE Transactions on Image Processing, 17, 1283-1294 (2007).

[40] Moreno, J.C., Prasath, V.B.S., Neves, J.C., Color image processing by vectorial total variation with gradient channels coupling. *Inverse Problems and Imaging* 10 (2), pp. 461-497 (2016)

[41] Melange, T., Zlokolica, V., Schulte, S., De Witte, V., Nachtegael, M., Pizurca, A., Kerre, E.E., Philips, W.: A new fuzzy motion and detail adaptive video filter- *Lecture Notes in Computer Science*, 4678, 640-651 (2007).

[42] De Backer, S., Pizurica, A., Huysmans, B., Philips, W., Scheunders, P.: Denoising of multicomponent images using wavelet least-squares estimators. *Image and Vision Computing*, 26, 1038-1051 (2008).

[43] Dengwen, Z., Wengang, C.: Image denoising with an optimal threshold and neighboring window- *Pattern Recognition Letters*, 29, 1694-1697 (2008).

[44] Schulte, S., Huysmans, B., Pizurica, A., Kerre, E.E., Philips, W.: A New Fuzzy-Based Wavelet Shrinkage Image Denoising Technique. *Proceedings of Advanced Conceptps for Intelligent Vision Systems ACIVS06, Lecture Notes in Computer Science*, 4179, 12-23 (2006).

[45] Pizurica, A., Philips, W.: Estimating the probability of the presence of a signal of interest in multiresolution single and multiband image denoising, *IEEE Transactions on Image Processing*, 15, 654-665 (2006).

[46] Scheunders, P.: Wavelet thresholding of multivalued images, *IEEE Transactions on Image Processing*, 13, 475-483 (2004).

[47] Sendur, L., Selesnick, I.W.: Bivariate shrinkage functions for wavelet-based denoising exploiting interscale dependency. *IEEE Transactions on Signal Processing*, 50, 2744-2756 (2002).

[48] Balster, E.J., Zheng, Y.F., Ewing, R.L.: Feature-based wavelet shrinkage algorithm for image denoising, *IEEE Transactions on Image Processing*, 14, 2024-2039 (2005).

[49] Miller, M., Kingsbury, N.: Image denoising using derotated complex wavelet coefficients. *IEEE Transactions on Image Processing*, 17, 1500-1511 (2008).

[50] Zhang, B., Fadili, J.M., Starck, J.L.: Wavelets, Ridgelets, and Curvelets for poisson noise removal.*IEEE Transactions on Image Processing*, 17, 1093-1108 (2008).

[51] Dabov, K., Foi, A., Katkovnik, V., Egiazarian, K.: Image denoising by sparse 3D transform-domain collaborative filtering, *IEEE Transactions on Image Processing*, 16, 2080-2095 (2007).

[52] Dabov, K., Foi, A., Katkovnik, V., Egiazarian, K.: Color image denoising via sparse 3D collaborative filtering with grouping constraint in luminance-chrominance space. *Proceedings of the IEEE International Conference on Image Processing* ICIP2007 , 313-316 (2007).

[53] Hao, B.B., Li, M., Feng, X.C.: Wavelet iterative regularization for image restoration with varying scale parameter. *Signal Processing: Image Communication*, 23, 433-441 (2008).

[54] Zhao, W., Pope, A.: Image restoration under significat additive noise. *IEEE Signal Processing Letters*, 14, 401-404 (2007).

[55] Gijbels, I., Lambert, A., Qiu, P.: Edge-preserving image denoising and estimation of discontinuous surfaces- *IEEE Transactions on Pattern Analysis and Machine Intelligence*, 28, 1075-1087 (2006).

[56] Liu, C., Szeliski, R., Kang, S.B., Zitnik, C.L.,Freeman, W.T.: Automatic estimation and removal of noise from a single image, *IEEE Transactions on Pattern Analysis and Machine Intelligente*, 30, 299-314 (2008).

[57] Jordan C., Morillas S., Sanabria-Codesal E.: Colour image smoothing through a soft-switching mechanism using a graph model, *IET Image Processing*, 6 (9),1293-1298 (2012).

[58] Bao, L., Song, Y., Yang, Q., Yuan, H., Wang, G., Tree filtering: Efficient structure-preserving smoothing with a minimum spanning tree. *IEEE Transactions on Image Processing* 23 (2), 6665130, pp. 555-569 (2014).

[59] Grecova, S.,Morillas, S.: Perceptual similarity between color images using fuzzy metrics. *J. Vis. Commun. Image R.*, 34, 230-235 (2016).

[60] Wang, Z., Bovik, A. C., Sheikh, H. R., Simoncelli. Image quality assessment: from error visibility to structural similarity. *IEEE transactions on image processing*, 13(4), 600-612 (2004).

[61] Immerkaer, J.: Fast Noise Variance Estimation. *Computer Vision and Image Understanding*, 64 (2), 300-302 (1996)

[62] Viola, P., Wells, W.M.: Alignment by maximization of mutual information. *International Journal of Computer Vision* 24 (2), 137-154, (1997).

[63] Maes F., Collingnon A., Vandermeulen, G. Marchal G., P. Suetens P.: Multimodality image registration by maximization of mutual information. *IEEE Transactions on Medial Imaging* 16 (2), 187-198 (1997).

[64] MathWorks. Fuzzy Logic Image Processing. https://es.mathworks.com/help /fuzzy/examples/fuzzy-logic-image-processing.html. Retrieved on November, 29th 2016.

[65] Lukac, R., Plataniotis, K. N. (2006). A taxonomy of color image filtering and enhancement solutions. *Advances in imaging and electron physics* , 140, 188.

[66] Celebi, E., Lecca, M., Smolka, B. (Eds.). (2015). Color Image and Video Enhancement. Springer International Publishing.